

Deep learning-based LSTM model for prediction of long-term piezoresistive sensing performance of cement-based sensors incorporating multi-walled carbon nanotube

Daeik Jang⁺¹, Jinho Bang⁺², H.N. Yoon¹, Joonho Seo¹, Jongwon Jung²,
Jeong Gook Jang^{*3} and Beomjoo Yang^{**2}

¹Department of Civil and Environmental Engineering, Korea Advanced Institute of Science and Technology,
291 Daehak-ro, Yuseong-gu, Daejeon 34141, Republic of Korea

²School of Civil Engineering, Chungbuk National University, 1 Chungdae-ro, Seowon-gu, Cheongju, Chungbuk 28644, Republic of Korea

³Division of Architecture and Urban Design, Urban Science Institute, Incheon National University,
119 Academy-ro, Yeonsu-gu, Incheon 22012, Republic of Korea

(Received July 4, 2022, Revised October 1, 2022, Accepted October 4, 2022)

Abstract. Cement-based sensors have been widely used as structural health monitoring systems, however, their long-term sensing performance have not actively investigated. In this study, a deep learning-based methodology is adopted to predict the long-term piezoresistive properties of cement-based sensors. Samples with different multi-walled carbon nanotube contents (0.1, 0.3, and 0.5 wt.%) are fabricated, and piezoresistive tests are conducted over 10,000 loading cycles to obtain the training data. Time-dependent degradation is predicted using a modified long short-term memory (LSTM) model. The effects of different model variables including the amount of training data, number of epochs, and dropout ratio on the accuracy of predictions are analyzed. Finally, the effectiveness of the proposed approach is evaluated by comparing the predictions for long-term piezoresistive sensing performance with untrained experimental data. A sensitivity of 6% is experimentally examined in the sample containing 0.1 wt.% of MWCNTs, and predictions with accuracy up to 98% are found using the proposed LSTM model. Based on the experimental results, the proposed model is expected to be applied in the structural health monitoring systems to predict their long-term piezoresistive sensing performances during their service life.

Keywords: deep-learning; long short-term memory; long-term cyclic loading; multi-walled carbon nanotube; piezoresistive sensors

1. Introduction

In the construction field, monitoring the long-term durability of structures throughout their service life is significant, and therefore considerable efforts have been made to monitor the soundness of structures efficiently (Lee *et al.* 2021, Dong *et al.* 2021). Recently, novel cement-based sensors capable of monitoring structural health have attracted attention (Abolhasani *et al.* 2022). For instance, conductive fillers have been added to a cement matrix to render the sensing capability to the matrix, simultaneously improving its structural durability (Park *et al.* 2021, Abolhasani *et al.* 2022). It has been widely reported that the electrical conductivity of the conductive fillers-added cement composites changes when external strain/stress is applied, indicating the piezoresistive properties (Bang *et al.* 2022). Based on these properties, many studies have investigated the sensing capability of conductive

cementitious composites. Chung (2002) fabricated cementitious composites by adding steel fibers, and tested their piezoresistive sensing properties. They observed the relationship between the fractional changes in electrical resistivity (FCR) and the amount of conductive fillers (Chung 2002). Sun *et al.* (2000) conducted the piezoresistive sensing tests using carbon fiber (CF)-reinforced concrete under dynamic loading conditions, which revealed that the fabricated concrete is sensitive to a large range of loads, showing the potential of being used as structural health monitoring (SHM) sensors.

Recently, many researchers have attempted to use carbon nanotubes (CNTs) instead of the conventional conductive fillers (e.g., carbon black, carbon fiber, graphite, and steel-based fibers), since the CNTs are nanoscale and have a high aspect ratio (Naeem *et al.* 2017, Wang *et al.* 2020, Zhang *et al.* 2018). These advantages of CNTs can generate outstanding conductive networks in cement matrix with a small amount compared to the conventional conductive fillers, improving both electrical and piezoresistive sensing properties. Jang *et al.* (2022) fabricated cement composites containing multi-walled CNTs (MWCNTs) and carbon black (CB) for piezoresistive sensors. Nam *et al.* (2017) manufactured cement-based sensors by incorporating a small amount of MWCNTs compared to previous works which used conventional

*Corresponding author, Ph.D.

E-mail: jangjg@inu.ac.kr

**Corresponding author, Ph.D.

E-mail: byang@cbnu.ac.kr

+These authors contributed equally to this work.

Table 1 Mix proportions of MWCNT/cement samples (wt.%)

Sample code	Cement	Silica fume	MWCNTs	Water	SP	Flow (mm)
C1	100	10	0.1	22	2.0	
C2	100	10	0.3	25	2.0	100±5
C3	100	10	0.5	28	2.0	

conductive fillers, exhibiting their sensing capability under the dynamic loading tests.

However, despite significant investigations on experimental studies about short-term sensing capabilities, it is difficult to examine their long-term sensing performances via experiments. This is because cement-based sensors are constantly subjected to continuous dynamic loading and damage as they are often exposed to outdoor environments, all of which can cause changes in their sensing performances (Gao *et al.* 2013, Zhao *et al.* 2014, Jang *et al.* 2022). Consequently, there are various limitations in experimentally analyzing the factors severely affecting cement-based sensors in a full range, thus, various efforts have been made to predict their piezoresistive sensing performances. For example, Garcia-Macias *et al.* (2018) proposed a micromechanics-integrated finite element (FE) multiphysics formulation for electromechanical modeling of a cementitious composite. Fang *et al.* (2021) derived an analytical model to simulate the influence of mechanical deformation on the electrical properties of CNTs-embedded composites, and the proposed model was validated by the experimental data obtained in the previous studies. In addition, Tallman and Wang (2013) presented a theoretical model that can predict the piezoresistive properties of CNTs-embedded composites under arbitrary straining, and they verified the accuracy of the proposed model by comparing their model with previous studies.

The above-mentioned previous studies addressed the numerical and theoretical methods for analyzing the piezoresistive properties of composites incorporating CNTs. However, the micromechanics- and/or FE-based theory has limitations for predicting the long-term degradation of the cementitious composites caused by fatigue, loading, or aging during their service life. These theoretical approaches can predict the piezoresistive sensing performance in a short time in the elastic stress-strain domain, however, these approaches may not be suitable for accurately predicting the long-term nonlinear behavior of infrastructures. Furthermore, the conventional approaches-based simulation is required to fit complex model parameters, which limits its suitability for engineering applications (Conti and O'Hagan 2010, Ongpeng *et al.* 2017). Whereas deep learning techniques are widely used to investigate complex systems in modern engineering problems, thus, a relatively efficient and reliable prediction method may be obtained by coupling long-term piezoresistive experimental data with deep-learning approaches (Yu *et al.* 2022a, Yu *et al.* 2022b). Although the investigations on long-term piezoresistive sensing performance of cement-based sensors were attempted, there has been little research into predicting such

long-term sensing stability. For these reasons, this study adopted a deep learning-based long short-term memory (LSTM) model to evaluate the prediction of long-term piezoresistive sensing performances of the cement-based sensors. The proposed model is expected to predict not only the long-term piezoresistive sensing performances of the cement-based sensors, but also the sensing stability as they are exposed to various weathering conditions.

In this study, cement-based sensors were fabricated using MWCNTs as conductive fillers, with three different concentrations (0.1, 0.3, and 0.5 wt.%). The electrical and sensing properties of the samples were investigated experimentally. Then, a deep learning-based LSTM model with three different input variables (time, MWCNTs content, and applied loading) and one output variable (fractional change in electrical resistivity, FCR) was adopted to predict the long-term piezoresistive sensing stability. In addition, numerical analysis was used to observe the suitable model parameters. Thereafter, the model was trained with 30% of the experimental data, and the remaining data were used to validate the predictions. Finally, the accuracy of the proposed model was evaluated in each cement-based sensor with different MWCNT contents.

2. Experiment and results

2.1 Sample preparation and experiment methods

Commercially available Type-I Portland cement (SAMPYO Cement Co., Ltd.) is used as the binder material in accordance with ASTM C150. MWCNTs with a diameter of 10 nm and length of 100-200 μm are incorporated into cementitious composites as conductive fillers. In addition, based on previous studies on methods of improving the dispersion of MWCNTs, 10 wt.% of silica fume (Elkem, Inc, EMS-970) and 2 wt.% of polycarboxylate-type SP (Dongnam Co., Ltd., FLOWMIX 3000L) are also incorporated (Yoon *et al.* 2020, Jang *et al.* 2021). Water-to-cement ratios (w/c) of 0.22-0.28 are used to maintain a target flow of 110±5 mm, which is regarded as a favorable flow ability for dispersing MWCNTs in cementitious composites (Jang *et al.* 2021). Samples with different MWCNT contents (0.1, 0.3, and 0.5 wt.%) are prepared, as the percolation threshold of MWCNT-embedded composites is an important factor in their electrical and piezoresistive sensing performances (Lim *et al.* 2021, Jang *et al.* 2022). Details of the mix proportions are presented in Table 1. The numbers in the sample code indicate the MWCNT content. For example, 1, 3, and 5 denote samples with 0.1, 0.3, and 0.5 wt.% of MWCNTs, respectively.

The samples are prepared as follows. First, cement, silica fume, and MWCNTs are placed in a Hobart mixer and mixed mechanically for 5 min at a low speed. Simultaneously, SP is added to the water. The solution containing water and SP is added to the dry mixtures (Park *et al.* 2019). Then, the mixtures are mixed mechanically for an additional 5 min at low speed, and 1 min at high speed. After mixing, the samples are placed in cubical molds (50×50×50 mm³). Copper electrodes (70 mm long and 20

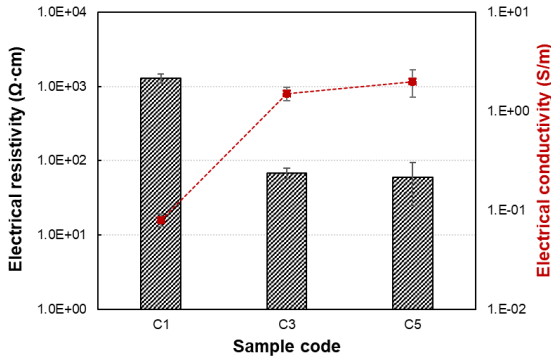


Fig. 1 Electrical resistivity and conductivity of samples

mm wide) are prepared, and both sides of the electrodes are coated with a silver paste to minimize the contact resistances between the samples and the electrodes. The prepared electrodes are embedded into the molds 20 mm apart and 50 mm deep. The samples are wrapped and cured in an oven at room temperature ($25 \pm 2^\circ\text{C}$) for 1 d. After 1 d, they are demolded, wrapped, and cured in the same oven for an additional 27 d to prevent undesired chemical reactions. After 28 d, the samples for the electrical conductivity and piezoresistive sensing tests are dried in an oven at 60°C for 3 d to evaporate any residual moisture.

A portable multimeter (Keysight, U1282A) is used to measure the electrical resistance of the samples. The two-probe method is used for convenience, and the measured electrical resistance is converted to electrical resistivity based on the dimensions of the electrodes. A servo-hydraulic universal testing machine (Walter Bai, LFV-2500HH) is used for the piezoresistive sensing test. Sinusoidal compressive loading between 0 and 50 kN and with a frequency of 2 Hz is applied to the samples for 10,000 cycles, and the corresponding electrical resistances of the samples are recorded using a digital multimeter (Agilent Technologies, DMM 34410A). The recorded electrical resistances are then converted to fractional resistance changes, as described in the previous study, using the following equation

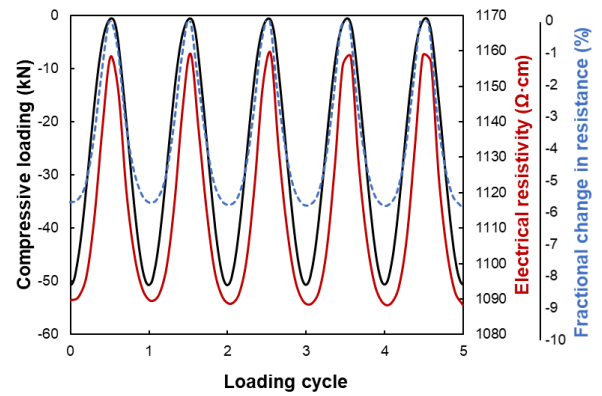
$$\text{FCR (\%)} = \frac{R_t - R_0}{R_0} \times 100 \quad (1)$$

where R_t denotes the electrical resistance at time t with compressive loading, and R_0 denotes the initial electrical resistance without an applied load.

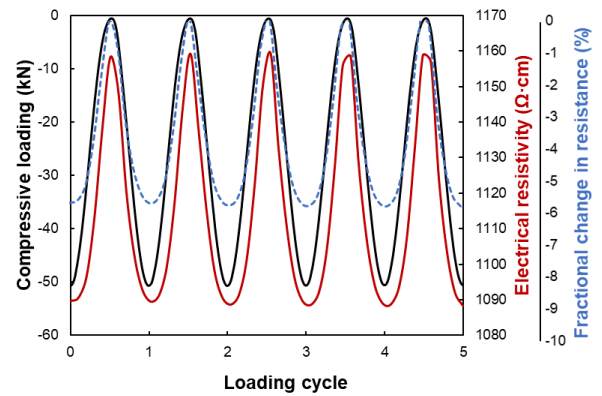
2.2 Piezoresistive sensing performance

The electrical resistivities and conductivities of the samples are shown in Fig. 1. The resistivities of samples C1, C3, and C5 are 1279.1, 68.4, and 59.0 $\Omega\cdot\text{cm}$, respectively. These values are converted to electrical conductivity, giving 0.08, 1.50, and 1.99 S/m, respectively.

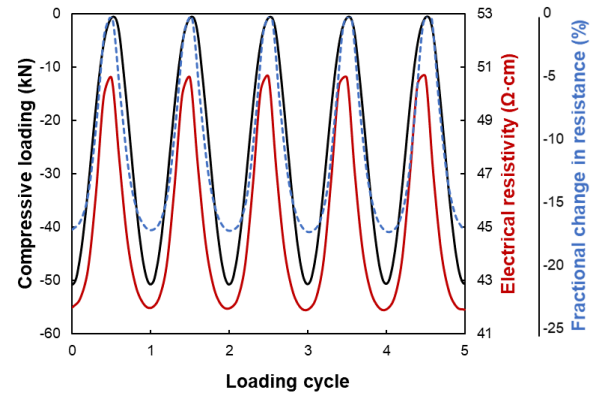
Fig. 1 shows that there are dramatic changes in the electrical resistivity and conductivity between samples C1 and C3, as the MWCNT content increases from 0.1% to 0.3%. This is called the percolation threshold (Jang *et al.* 2022). As reported in previous studies, the percolation threshold of CNT/cement composites is approximately 0.3-



(a)



(b)



(c)

Fig. 2 Piezoresistive sensing performances of samples (a) C1, (b) C3, and (c) C5 during cyclic loading

0.5% MWCNT content by cement mass. The percolation threshold obtained in this study is equal to or less than that found in previous studies, indicating that the MWCNTs are well dispersed in the composites. Fig. 2 shows the piezoresistive sensing performance of the samples during the cyclic loading tests. It can be seen that the electrical resistivity decreases as the applied compressive load increases.

This occurs due to changes in the distance between adjacent MWCNT particles. When a load is applied to the composites, the distance between adjacent MWCNTs decreases, thus the electrical resistivity decreases. This is called the piezoresistive sensing principle (Khalid *et al.* 2021, Bhandari *et al.* 2021, Jang *et al.* 2021). Based on the

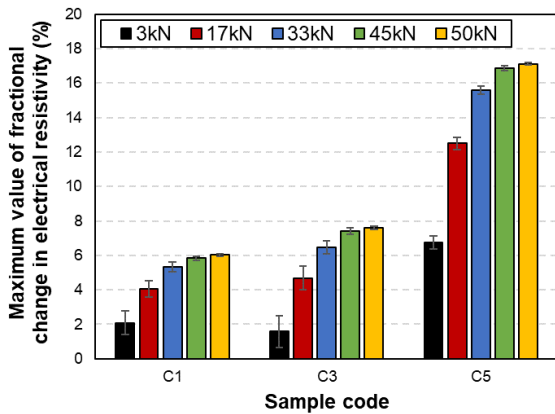


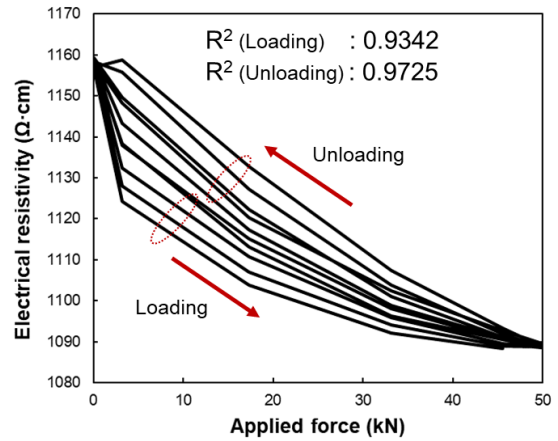
Fig. 3 Maximum fractional change in electrical resistivity of samples during cyclic loading test

piezoresistive sensing performance results shown in Fig. 2, the maximum FCR under representative compressive loading is shown in Fig. 3. Samples C1 and C3 show similar results, with approximately 6% and 8% of the maximum FCR value when a 50 kN compressive load is applied to the samples. Sample C5 shows approximately 17% of the maximum FCR under the same conditions.

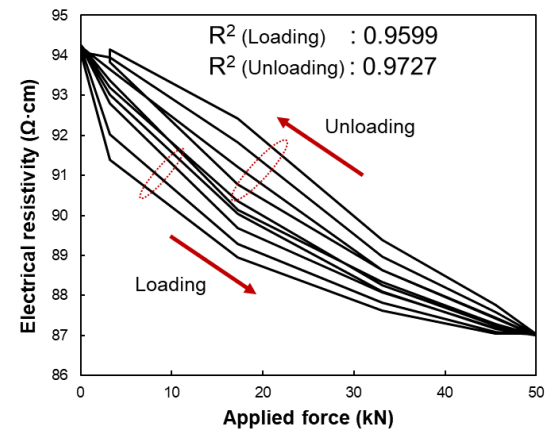
This result can be explained by the percolation threshold, as described above. In sample C1, where the MWCNT content is below the percolation threshold (<0.3 wt.%), the MWCNT particles are too sparse to form effective conductive networks. The conductive networks improve as the MWCNT content increases above the percolation threshold (i.e., 0.3-0.5 wt.%) and contact between adjacent MWCNT particles increases. This is the reasonable reason of sample C5 has a higher FCR than samples C1 and C3. In addition, sample C5 shows approximately 7% of the maximum FCR value when a 3 kN compressive load is applied, whereas samples C1 and C3 show less than 2% of the maximum FCR. This result is also supported by the above explanation, as a reduction in the compressive load may not reduce the distance between adjacent MWCNT particles, resulting in lower sensitivity.

Repeatability is another important factor in piezoresistive sensing performance, and it is related to sensing stability. Here, the repeatability of the piezoresistive sensing performance is expressed as R -squared (R^2), as shown in Fig. 4. The R^2 values are calculated separately under loaded and unloaded conditions to avoid the effects of hysteresis, which occurs during cyclic loading (Yu *et al.* 2016). The R^2 values of samples C1, C3, and C5 are 0.9342, 0.9599, and 0.9987, respectively, under loaded conditions, and 0.9725, 0.9727, and 0.9985, respectively, under unloaded conditions.

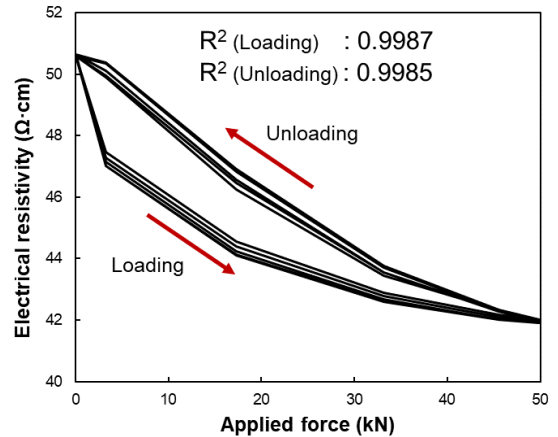
The R^2 value is lower in the loaded condition because micro-cracks developed and disrupted the conductive network, lowering the sensing stability. In particular, the R^2 values increase as the embedded MWCNT content increases from 0.1 to 0.5 wt.%. As explained above, the conductive networks are densest in sample C5. This meant that the disruption of individual MWCNTs during cyclic loading has less effect on sample C5 than on samples C1 and C3.



(a)



(b)



(c)

Fig. 4 Piezoresistive sensing stability of samples (a) C1, (b) C3, and (c) C5 expressed as R -squared

The response time for piezoresistive sensing is also investigated, and the peak shift properties are used to compare the response times of the samples. The peak shift indicates the time interval between the moment of maximum compressive loading and electrical resistivity, as illustrated in Fig. 5. Accordingly, the composites respond more rapidly as the time interval decreases. The calculated peak shift values are shown in Fig. 5(b), and are approximately 6.2%, 5.8%, and 4.0% for samples C1, C3, and C5, respectively.

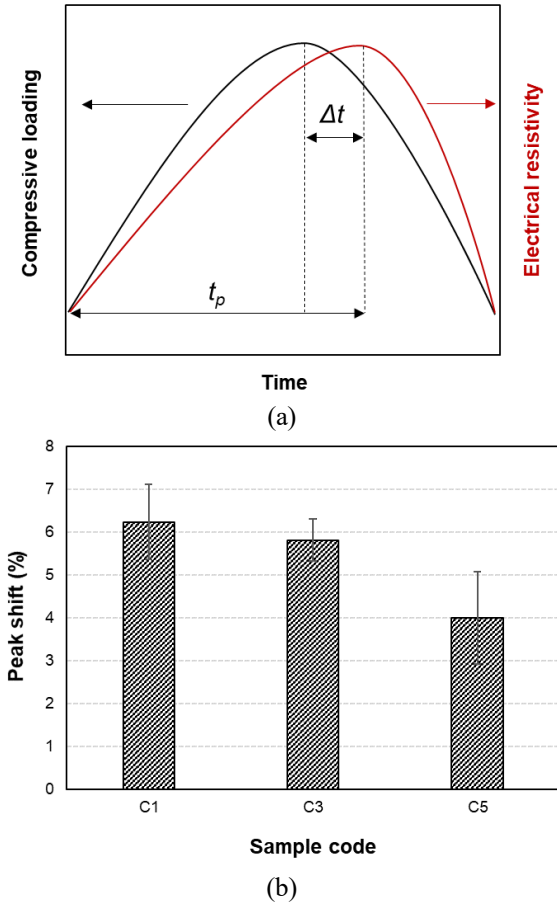


Fig. 5 (a) Schematic description of response time expressed as peak shift and (b) peak shift values of samples obtained from the cyclic loading test

The obtained peak shift values agree well with the electrical characteristics, as shown in Fig. 1. The distance between adjacent MWCNTs decreases as the quantity of embedded MWCNTs increases, and denser conductive networks are formed (Yang *et al.* 2014, Nie *et al.* 2022). Consequently, the sample with the highest MWCNT content has the fastest response when a compressive load is applied. From the piezoresistive sensing performance results, it can be found that the samples with MWCNT contents above the percolation threshold (i.e., 0.5 wt.%) are suitable for use as piezoresistive sensors because of their high sensitivity (FCR), good sensing stability (R^2), and fast response (Peak shift).

3. LSTM model for prediction of long-term piezoresistive sensing performance

3.1 Recapitulation of LSTM model

To assess the potential of the deep learning technique for time-dependent simulations of samples, a long short-term memory (LSTM) network is adopted in the present study. Recurrent neural networks (RNNs) are a basic concept in deep learning, and they consist of artificial neural network models with a structure continuously connected by nodes,

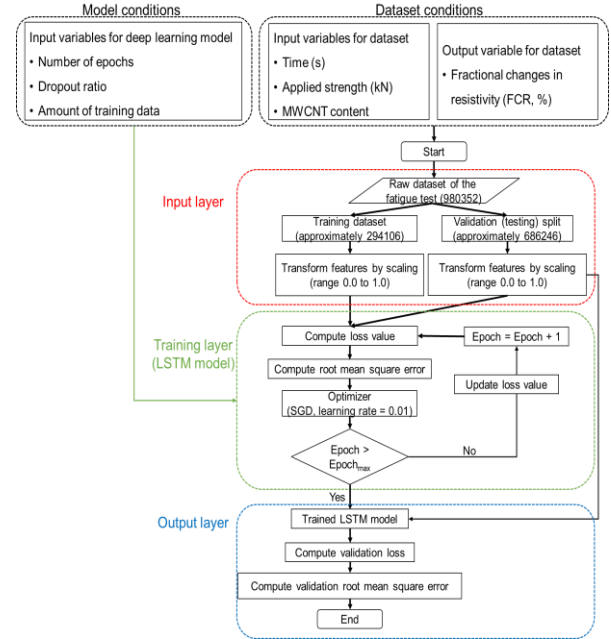


Fig. 6 Flowchart of the proposed workflow for assessing the effect of calibration data on the performance of different models

Table 2 Components of deep learning in LSTM method

Index	Components
Software	Tensorflow
Model of LSTM	BasicLSTMCell
Learning rate	0.01
Epoch	10 - 100
Dense	1.0
Dropout ratio	0.1 - 0.9
Batch size	32
Data scaling	MinMaxScaler
Input variables	Time (s) Contents of CNTs (wt.%) Applied stress (kN)
Output variable	Fractional change in electrical resistivity (FCR, %)

similar to neurons. They can control the sequential length of a variable using the feedforward method for user convenience (Graves *et al.* 2013, Asteris *et al.* 2021). An RNN updates the hidden layer using the equation

$$h_t = g(W_{xh}x_t + W_{hh}h_{t-1} + b_h) \quad (2)$$

where the input data x enters the layer, the feature is determined by the weight function W and bias b . The output data h can be obtained by multiplying this by the hidden layer function g , in addition to the tangent hyperbolic function (Berradi and Lazaar 2019).

However, in previous studies using data with long-term dependence, problems occur where the weights suddenly explode or disappear when backpropagation is adopted with learning algorithms based on RNNs (Bengio *et al.* 1994). LSTM is a modified RNN designed to overcome these limitations, and it shows outstanding performance compared with other traditional models, especially with

long-term dependent data such as speech recognition, translation, and language modeling (Kratzert *et al.* 2018, Nguyen *et al.* 2019). LSTM has an additional advantage in terms of its ability to memorize the sequence of data. Memorization of earlier trends in the data is possible through three gates, combined with a memory line incorporated in a typical LSTM system.

LSTM can be trained reliably through long-term dependencies where each layer exchanges information with the others. The cell state, one of the major differences between LSTM and traditional RNNs, can operate the entire LSTM system with simple linear calculations and transfer long-term data stored in the memory without deformation. The cell state is composed of three gates: (1) input, (2) output, and (3) forget. The LSTM adopted in this study investigates the performance to difference in the states with the same detailed settings (Karim *et al.* 2017, Yadav *et al.* 2020), therefore, the default values provided by BasicLSTMCell (Castangia *et al.* 2021) were applied in the present study except for the changes in the hyperparameter values listed in Table 2. According to previous studies (Cai *et al.* 2020, Liu *et al.* 2019), it can be found that the noise-induced sensitivity can be adjusted by adopting hyperparameter tuning process. Future research plans to supplement these defects and propose a more practical model. Further details are described in Table 2, and an outline of the simulation is shown in Fig. 6 as a flow chart.

3.2 Parametric analysis and piezoresistive predictions

In this study, the root-mean-square error (RMSE) is used to evaluate the performance of the proposed deep learning model. The LSTM model uses the 980352, 980802, and 999832 of datasets to train the neural net and validate predictions for samples C1, C3, and C5, respectively. Fig. 7 displays the adopted dataset with 10,000 cycles for all the samples. The datasets include four variables: the quantity of MWCNTs, time, electrical resistivity, and applied stress. Whereas the LSTM-based simulation parameters include the learning rate, number of epochs, and dropout ratio. Herein, the learning rate signifies how quickly the training process converges (Mohammadhassani *et al.* 2013, Yu *et al.* 2020). The number of epochs means the number of executions, and in general, the accuracy improves as the number of epochs increases, however, increasing the number of epochs considerably increases the computational resources and time required.

Dropout is a learning method that arbitrarily deletes neurons, and users can arbitrarily set the ratio of neurons to be deleted (Yu *et al.* 2020). In general, the learning rate is an effective variable in solving the overfitting and underfitting of prediction, in this study, it is fixed and applied to the experiment. A parametric study is conducted to examine the effects of these parameters with a control group and a comparison group. The results of these experiments are presented in Fig. 7, and the predictions are compared to the untrained experimental data to assess the predictive capability of the proposed deep learning-based model. The LSTM simulation is used to predict the FCR of the MWCNT/cement composites with various model parameters: the amount of training data, dropout ratio, and

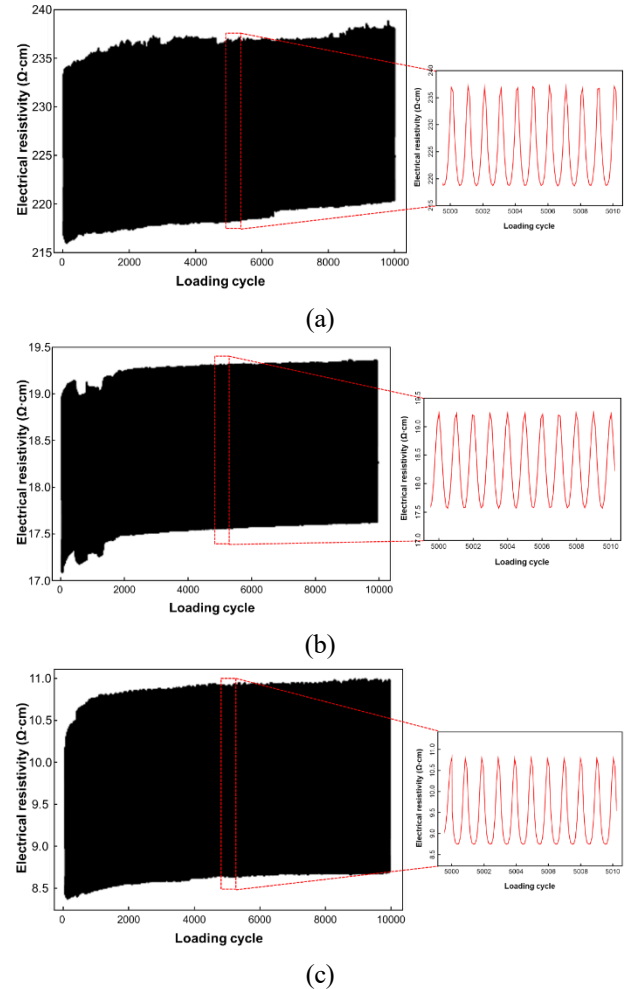


Fig. 7 Experimental results for adopted dataset with 10 000 cycles of samples (a) C1, (b) C2, and (c) C3

number of epochs.

The datasets are preprocessed for more accurate predictions and comparisons using MinMaxScaler. The C1 dataset is considered for an initial investigation of the model parameters. It shows that the best fit for C1 is obtained when 50% of the dataset is used for training, the dropout ratio is 0.3, and the system runs for 50 epochs. The fastest test uses 30% of the dataset for training, a dropout ratio of 0.3, and runs for 10 epochs.

The RMSE of the training and test errors are used to evaluate the effect of the size of the training dataset. Considering the amount of training data, the learning rate, epoch, and batch size are set to 0.01, 50, and 32, respectively. Subsequently, 5%, 10%, 30%, and 50% of the total data for C1 are utilized for training, and validation is based on the remaining data. The RMSE results, in accordance with the number of epochs, are shown in Fig. 8. As the amount of training data increases, the RMSE values converge more rapidly. That is, when 5% of the dataset is used for training, it converges to the final result after approximately 10 epochs.

In contrast, when 10% or 30% of the dataset is used for training, it converges after 6 and 3 epochs, respectively. Furthermore, when 50% of the dataset is used for training,

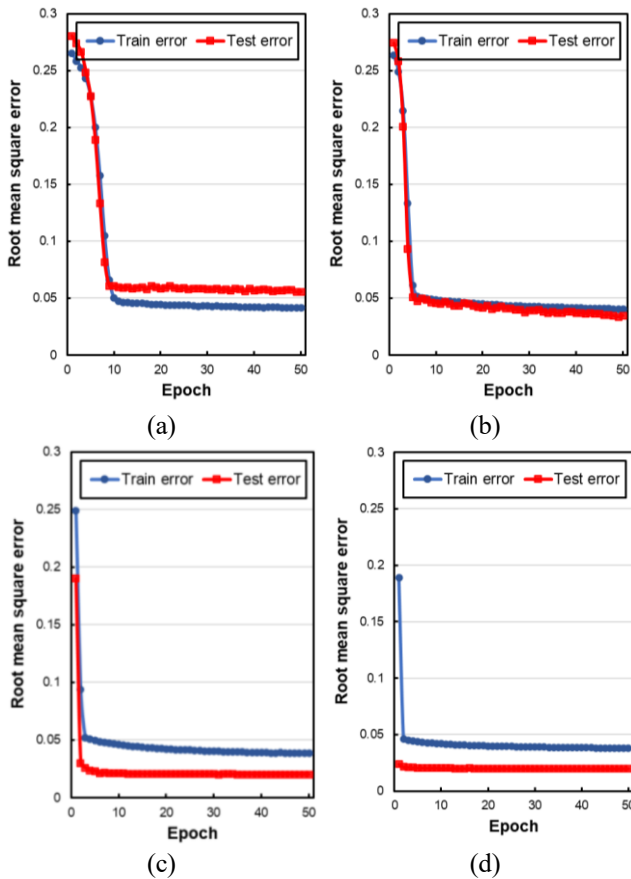


Fig. 8 Root mean square error with (a) 5%, (b) 10%, (c) 30%, and (d) 50% of the experimental dataset used for training

the first simulation is similar to the final result. Overall, the epochs during the simulation process and the simulation time increased, however, a linear causal relationship could not be confirmed.

Fig. 9 shows a comparison between the actual value (ground truth) and prediction for various dropout ratios. To examine the effect of dropout ratio, which prevents overfitting in the learning processes, a parametric study is conducted with various dropout values. Furthermore, to evaluate the effect of the weight parameter, three variables are set, as above. As the dropout ratio decreases, the prediction result is fitted more accurately. However, when the dropout ratio became extremely small, it is confirmed that the time almost doubled. Fig. 10 shows a comparison of the actual and predicted values after 10, 50, and 100 epochs.

To confirm the results more specifically, the predicted and actual values for cycles 4500-4504 are considered. The predicted values generally converge within 10 epochs, so there is no significant difference, however, as the number of epochs increases, the variation between the predicted values and the actual values decreases. Compared to the amount of training data and dropout ratio, the number of epochs does not have a significant effect.

The LSTM-based simulation results based on the C1 dataset show that it may be appropriate to use 30% of the dataset for training, a dropout ratio of 0.3, and 50 epochs. The accuracy and computational cost of the analysis are

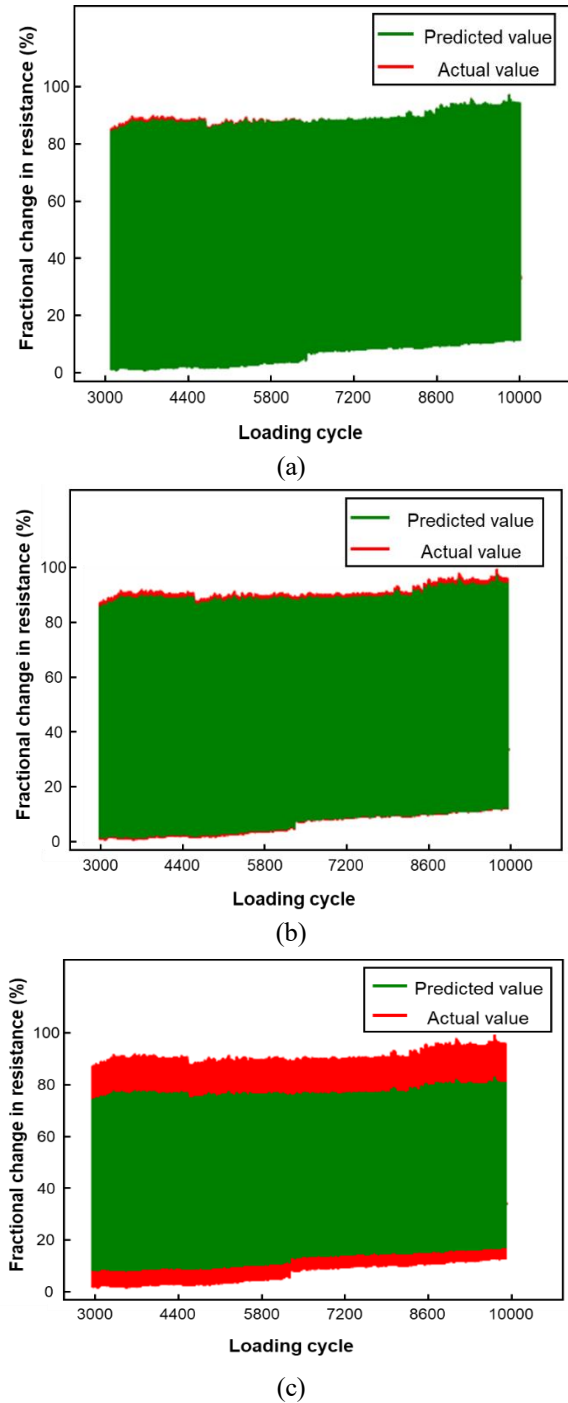


Fig. 9 Comparison of actual and predicted values with dropout ratios of (a) 0.1, (b) 0.3, and (c) 0.9

considered, and the same parameters are applied to the data for samples C3 and C5.

Fig. 11 shows the training and validation datasets used to examine the RMSE of the predictions based on the LSTM model. Here, 30% of the total dataset is used for training, and the rest is used to validate the predicted value. Overall, there is no significant difference in the values, however, the expected result for C1 has a slightly lower RMSE than that for C3, which is supposed to have noise in the training dataset, and C5, in which the validation dataset is considered to be flat. The main results of this study

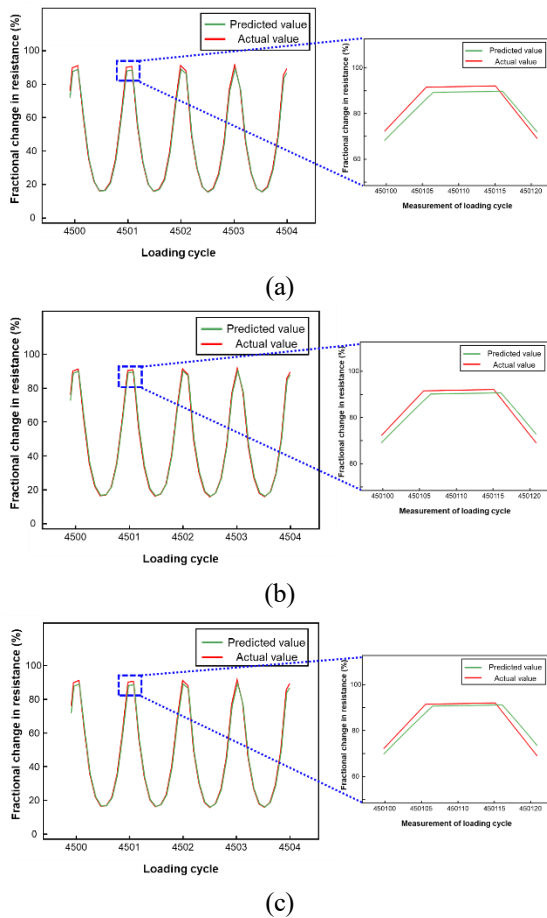


Fig. 10 Comparison of actual and predicted values after (a) 10, (b) 50, and (c) 100 epochs for specific loading cycles

Table 3 Results with time calculated using LSTM method

Output variable	Sample code	Dropout ratio	Epoch	Amount of data (%)	RMSE	Required time (s)
FCR (%)	C1	0.1	50	30	0.0199	6205.563
			10	30	0.0210	805.721
		0.3	5	0.0447	2305.396	
			10	0.0257	2725.250	
			30	0.0202	3639.966	
			50	0.0199	4733.435	
	0.9	100	0.0201	7405.863		
		50	0.0643	3475.401		
	C2	0.3	50	30	0.0204	2757.071
	C3				0.0205	3330.604

including the effects of the amount of training data, dropout ratio, and number of iterations are presented in Table 3.

4. Conclusions

Cement-based sensors are exposed to continuous dynamic loading and/or damage, degrading their sensing stability, nevertheless, predictions of long-term sensing stability have rarely been reported. Therefore, this study presents a deep-learning analysis combining experimental

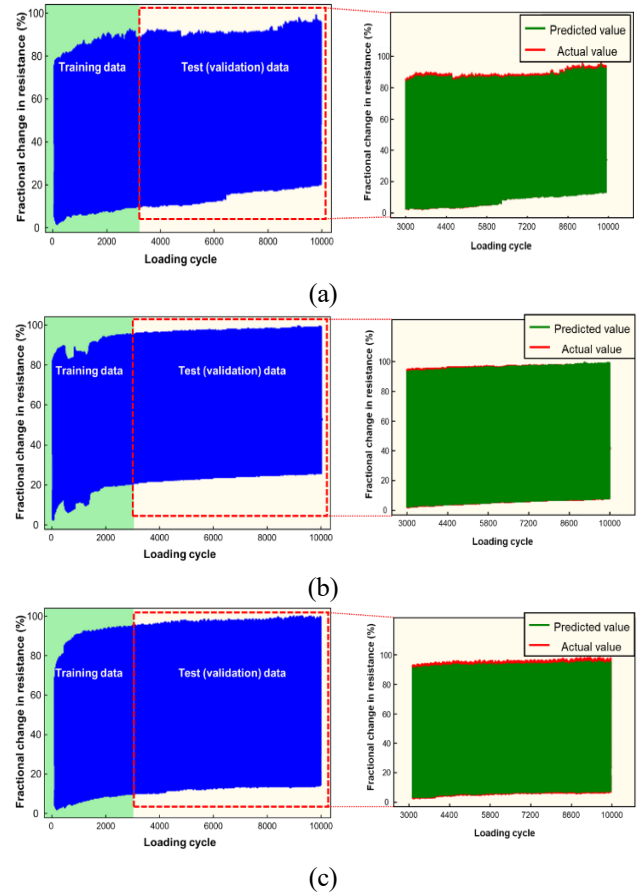


Fig. 11 Comparison of actual and predicted values with MWCNT contents of (a) 0.1 wt.%, (b) 0.3 wt.%, and (c) 0.5 wt.%

data and a LSTM model to predict the stability of long-term piezoresistivity. Related experiments are conducted, and the test results are used as training data. The simulations indicate that the parameters of the LSTM model have a notable effect on the predicted long-term piezoresistive sensing performances of the composites. By comparing the predictions with the experimental results, the validity of the proposed deep-learning approach is evaluated, and the following conclusions can be drawn from this study.

- The electrical resistivity decreases from 1279.1 to 59.5 $\Omega \cdot \text{cm}$ as the embedded MWCNT content increases from 0.1 to 0.5 wt.%. For the piezoresistive sensing results, the sample with 0.5 wt.% of MWCNTs, which is within the range of the percolation threshold, shows the highest FCR of 17%.
- When a cyclic load is applied continuously, the FCR of the samples tends to be higher than that in the initial period. Samples with 0.5 wt.% of MWCNTs show the most stable long-term piezoresistive sensing behavior.
- The LSTM-based predictions are significantly affected by the model parameters, such as the quantity of training data, dropout ratio, and number of epochs. The optimal prediction results are obtained when the 30% of the total dataset is used for training, the dropout ratio is 0.3, and there are 50 epochs.
- To validate of the proposed deep learning approach,

30% of the total dataset is used to train the LSTM, and the piezoresistive sensing performance is predicted for the remaining 70%. The average RMSE is 0.02, and the average calculation time is approximately 1.14 h, which is 18% less than the time consumed by long-term piezoresistive sensing.

These findings are expected to contribute to predict the long-term sensing stability of cement-based sensors by considering the complex properties of cement, long-term behaviors, and mechanical-electrical relations. However, there have some imitations of the proposed model to apply in various types of cement-based sensors considering the external environmental conditions, thus, further studies will be carried out to improve the accuracy and mitigate the drawbacks of the proposed models. In addition, the proposed model will be applied to predict the sensing performances of cement-based sensors as they are exposed to various weathering conditions.

Acknowledgments

This work was supported by the National Research Foundation of Korea grant funded by the Korean government (MSIT) (2020R1C1C1005063 and 2022R1A4A3029737). In addition, this study was supported by a grant (21CTAP-C163988-01) from Ministry of Land, Infrastructure and Transport (MOLIT) of Korea government and Korea Agency for Infrastructure Technology Advancement (KAIA).

References

- Abolhasani, A., Pachenari, A., Razavian, S.M. and Abolhasani, M.M. (2022), "Towards new generation of electrode-free conductive cement composites utilizing nano carbon black", *Constr. Build. Mater.*, **323**, 126576. <https://doi.org/10.1016/j.conbuildmat.2022.126576>.
- Asteris, P.G., Apostolopoulou, M., Skentou, A.D. and Moropoulou, A. (2019), "Application of artificial neural networks for the prediction of the compressive strength of cement-based mortars", *Comput. Concrete*, **24**(4), 329-345. <https://doi.org/10.12989/cac.2019.24.4.329>.
- Bang, J., Bae, J.H., Jung, J. and Yang, B. (2022), "A short review of the literature on the multiscale modeling of nanoparticle-reinforced composites", *Multisc. Sci. Eng.*, **4**, 94-101. <https://doi.org/10.1007/s42493-022-00083-y>.
- Bengio, Y., Simard, P. and Frasconi, P. (1994), "Long-term dependencies with gradient descent is difficult", *IEEE Trans. Neur. Net.*, **5**(2), 157-166. <https://doi.org/10.1109/72.279181>.
- Berradi, Z. and Lazaar, M. (2019), "Integration of principal component analysis and recurrent neural network to forecast the stock price of casablanca stock exchange", *Procedia Comput. Sci.*, **148**, 55-61. <https://doi.org/10.1016/j.procs.2019.01.008>.
- Bhandari, M., Wang, J., Jang, D., Nam, I. and Huang, B. (2021), "A comparative study on the electrical and piezoresistive sensing characteristics of GFRP and CFRP composites with hybridized incorporation of carbon nanotubes, graphenes, carbon nanofibers, and graphite nanoplatelets", *Sensor.*, **21**(21), 7291. <https://doi.org/10.3390/s21217291>.
- Cai, L., Lei, M., Zhang, S., Yu, Y., Zhou, T. and Qin, J. (2020), "A noise-immune LSTM network for short-term traffic flow forecasting. Chaos: An Interdisciplinary", *J. Nonlin. Sci.*, **30**(2), 023135. <https://doi.org/10.1063/1.5120502>.
- Castangia, M., Aliberti, A., Bottaccioli, L., Macii, E. and Patti, E. (2021), "A compound of feature selection techniques to improve solar radiation forecasting", *Exp. Syst. Appl.*, **178**, 114979. <https://doi.org/10.1016/j.eswa.2021.114979>.
- Chung, D.D.L. (2002), "Piezoresistive cement-based materials for strain sensing", *J. Intell. Mater. Syst. Struct.*, **13**(9), 599-609. <https://doi.org/10.1106/104538902031861>.
- Conti, S. and O'Hagan, A. (2010), "Bayesian emulation of complex multi-output and dynamic computer models", *J. Stat. Plan. Inference.*, **140**(3), 640-651. <https://doi.org/10.1016/j.jspi.2009.08.006>.
- Dong, W., Li, W., Zhu, X., Sheng, D. and Shah, S. P. (2021), "Multifunctional cementitious composites with integrated self-sensing and hydrophobic capacities toward smart structural health monitoring", *Cement Concrete Compos.*, **118**, 103962. <https://doi.org/10.1016/j.cemconcomp.2021.103962>.
- Fang, Y., Li, L.Y. and Jang, S.H. (2021), "Piezoresistive modelling of CNTs reinforced composites under mechanical loadings", *Compos. Sci. Technol.*, **208**, 108757. <https://doi.org/10.1016/j.compscitech.2021.108757>.
- Gao, J., Yu, Z., Song, L., Wang, T. and Wei, S. (2013), "Durability of concrete exposed to sulfate attack under flexural loading and drying-wetting cycles", *Constr. Build. Mater.*, **39**, 33-38. <https://doi.org/10.1016/j.conbuildmat.2012.05.033>.
- García-Macias, E., Castro-Triguero, R., Sáez, A. and Ubertini, F. (2018), "3D mixed micromechanics-FEM modeling of piezoresistive carbon nanotube smart concrete", *Comput. Methods Appl. Mech. Eng.*, **340**, 396-423. <https://doi.org/10.1016/j.cma.2018.05.037>.
- Graves, A., Mohamed, A.R. and Hinton, G. (2013), "Speech recognition with deep recurrent neural networks", *2013 IEEE International Conference on Acoustics, Speech and Signal Processing*, May.
- Guerra, V., Wan, C. and McNally, T. (2020), "Fused deposition modelling (FDM) of composites of graphene nanoplatelets and polymers for high thermal conductivity: A mini-review", *Funct. Compos. Mater.*, **1**(1), 1-11. <https://doi.org/10.1186/s42252-020-00005-x>.
- Jang, D., Farooq, S.Z., Yoon, H.N. and Khalid, H.R. (2021), "Design of a highly flexible and sensitive multi-functional polymeric sensor incorporating CNTs and carbonyl iron powder", *Compos. Sci. Technol.*, **207**, 108725. <https://doi.org/10.1016/j.compscitech.2021.108725>.
- Jang, D., Yoon, H. N., Seo, J. and Park, S. (2022), "Enhanced electrical heating capability of CNT-embedded cementitious composites exposed to water ingress with addition of silica aerogel", *Ceram. Int.*, **48**(9), 13356-13365. <https://doi.org/10.1016/j.ceramint.2022.01.216>.
- Jang, D., Yoon, H. N., Seo, J. and Yang, B. (2022), "Effects of exposure temperature on the piezoresistive sensing performances of MWCNT-embedded cementitious sensor", *J. Build. Eng.*, **47**, 103816. <https://doi.org/10.1016/j.jobte.2021.103816>.
- Jang, D., Yoon, H.N., Seo, J., Cho, H.J., Kim, G.M., Kim, Y.K. and Yang, B. (2022), "Improved electromagnetic interference shielding performances of carbon nanotube and carbonyl iron powder (CNT@ CIP)-embedded polymeric composites", *J. Mat. Res. Tech.*, **18**, 1256-1266. <https://doi.org/10.1016/j.jmrt.2022.02.134>.
- Jang, D., Yoon, H.N., Seo, J., Lee, H.K. and Kim, G.M. (2021), "Effects of silica aerogel inclusion on the stability of heat generation and heat-dependent electrical characteristics of cementitious composites with CNT", *Cement Concrete Compos.*, **115**, 103861. <https://doi.org/10.1016/j.cemconcomp.2020.103861>.
- Jang, D., Yoon, H.N., Yang, B., Seo, J., Farooq, S.Z. and Lee, H.K. (2022), "Synergistic effects of CNT and CB inclusion on the

- piezoresistive sensing behaviors of cementitious composites blended with fly ash”, *Smart Struct. Syst.*, **29**(2), 351-359. <https://doi.org/10.12989/sss.2022.29.2.351>.
- Karim, F., Majumdar, S., Darabi, H. and Chen, S. (2017), “LSTM fully convolutional networks for time series classification”, *IEEE Access*, **6**, 1662-1669. <https://doi.org/10.1109/access.2017.2779939>.
- Khalid, H.R., Choudhry, I., Jang, D., Abbas, N., Haider, M.S. and Lee, H.K. (2021), “Facile synthesis of sprayed CNTs layer-embedded stretchable sensors with controllable sensitivity”, *Polym.*, **13**(2), 311. <https://doi.org/10.3390/polym13020311>.
- Kratzert, F., Klotz, D., Brenner, C., Schulz, K. and Hermegger, M. (2018), “Rainfall-runoff modelling using long short-term memory (LSTM) networks”, *Hydrol. Earth Syst. Sci.*, **22**(11), 6005-6022. <https://doi.org/10.5194/hess-22-6005-2018>.
- Kratzert, F., Klotz, D., Shalev, G., Klambauer, G., Hochreiter, S. and Nearing, G. (2019), “Towards learning universal, regional, and local hydrological behaviors via machine learning applied to large-sample datasets”, *Hydrol. Earth Syst. Sci.*, **23**(12), 5089-5110. <https://doi.org/10.5194/hess-23-5089-2019>.
- Lee, S.J., You, I., Kim, S., Shin, H.O. and Yoo, D.Y. (2022), “Self-sensing capacity of ultra-high-performance fiber-reinforced concrete containing conductive powders in tension”, *Cement Concrete Compos.*, **125**, 104331. <https://doi.org/10.1016/j.cemconcomp.2021.104331>.
- Lehky, D., Lipowczan, M., Simonova, H. and Kersner, Z. (2021), “A hybrid artificial neural network-based identification system for fine-grained composites”, *Comput. Concrete*, **28**(4), 369-378. <https://doi.org/10.12989/cac.2021.28.4.369>.
- Lim, H.J., Choi, H., Yoon, S.J., Lim, S.W., Choi, C.H. and Yun, G.J. (2021), “Micro-CT image-based reconstruction algorithm for multiscale modeling of Sheet Molding Compound (SMC) composites with experimental validation”, *Compos. Mater. Eng.*, **3**(3), 221-239. <https://doi.org/10.12989/cme.2021.3.3.221>.
- Liu, F., Cai, M., Wang, L. and Lu, Y. (2019), “An ensemble model based on adaptive noise reducer and over-fitting prevention LSTM for multivariate time series forecasting”, *IEEE Access*, **7**, 26102-26115. <https://doi.org/10.1109/access.2019.2900371>.
- Mohammadhassani, M., Nezamabadi-Pour, H., Jumaat, M.Z., Jameel, M. and Arumugam, A. (2013), “Application of artificial neural networks (ANNs) and linear regressions (LR) to predict the deflection of concrete deep beams”, *Comput. Concrete*, **11**(3), 237-252. <https://doi.org/10.12989/cac.2013.11.3.237>.
- Naeem, F., Lee, H.K., Kim, H.K. and Nam, I.W. (2017), “Flexural stress and crack sensing capabilities of MWNT/cement composites”, *Compos. Struct.*, **175**, 86-100. <https://doi.org/10.1016/j.compstruct.2017.04.078>.
- Nam, I.W., Souri, H. and Lee, H.K. (2016), “Percolation threshold and piezoresistive response of multi-wall carbon nanotube/cement composites”, *Smart Struct. Syst.*, **18**(2), 217-231. <https://doi.org/10.12989/sss.2016.18.2.217>.
- Nguyen, T.N., Yu, Y., Li, J., Gowripalan, N. and Sirivivatnanon, V. (2019), “Elastic modulus of ASR-affected concrete: An evaluation using Artificial Neural Network”, *Comput. Concrete*, **24**(6), 541-553. <https://doi.org/10.12989/cac.2019.24.6.541>.
- Nie, F., Chow, C.L. and Lau, D. (2022), “A review on multiscale modeling of asphalt: Development and applications”, *Multisc. Sci. Eng.*, **3**(3-4), 1-18. <https://doi.org/10.1007/s42493-022-00076-x>.
- Ongpeng, J., Soberano, M., Oreta, A. and Hirose, S. (2017), “Artificial neural network model using ultrasonic test results to predict compressive stress in concrete”, *Comput. Concrete*, **19**(1), 59-68. <https://doi.org/10.12989/cac.2017.19.1.059>.
- Park, H.M., Park, S., Shon, I.J., Kim, G.M., Hwang, S., Lee, M.W. and Yang, B. (2021), “Influence of Portland cement and alkali-activated slag binder on the thermoelectric properties of the p-type composites with MWCNT”, *Constr. Build. Mater.*, **292**, 123393. <https://doi.org/10.1016/j.conbuildmat.2021.123393>.
- Park, H.M., Park, S.M., Lee, S.M., Shon, I.J., Jeon, H. and Yang, B.J. (2019), “Automated generation of carbon nanotube morphology in cement composite via data-driven approaches”, *Compos. Part B: Eng.*, **167**, 51-62. <https://doi.org/10.1016/j.compositesb.2018.12.011>.
- Sun, M., Liu, Q., Li, Z. and Hu, Y. (2000), “A study of piezoelectric properties of carbon fiber reinforced concrete and plain cement paste during dynamic loading”, *Cement Concrete Res.*, **30**(10), 1593-1595. [https://doi.org/10.1016/S0008-8846\(00\)00338-0](https://doi.org/10.1016/S0008-8846(00)00338-0).
- Tallman, T. and Wang, K.W. (2013), “An arbitrary strains carbon nanotube composite piezoresistivity model for finite element integration”, *Appl. Phys. Lett.*, **102**(1), 011909. <https://doi.org/10.1063/1.4774294>.
- Wang, Y., Zhao, X. and Zhao, Y. (2020), “Piezoresistivity of cement matrix composites incorporating multiwalled carbon nanotubes due to moisture variation”, *Adv. Civil Eng.*, **2020**, Article ID 5476092. <https://doi.org/10.1155/2020/5476092>.
- Yadav, A., Jha, C.K. and Sharan, A. (2020), “Optimizing LSTM for time series prediction in Indian stock market”, *Procedia Comput. Sci.*, **167**, 2091-2100. <https://doi.org/10.1016/j.procs.2020.03.257>.
- Yang, B.J., Souri, H., Kim, S., Ryu, S. and Lee, H.K. (2014), “An analytical model to predict curvature effects of the carbon nanotube on the overall behavior of nanocomposites”, *J. Appl. Phys.*, **116**(3), 033511. <https://doi.org/10.1063/1.4890519>.
- Yoon, H.N., Jang, D., Lee, H.K. and Nam, I.W. (2021), “Influence of carbon fiber additions on the electromagnetic wave shielding characteristics of CNT-cement composites”, *Constr. Build. Mater.*, **269**, 121238. <https://doi.org/10.1016/j.conbuildmat.2020.121238>.
- Yu, C., Qi, X., Ma, H., He, X., Wang, C. and Zhao, Y. (2020), “LLR: Learning learning rates by LSTM for training neural networks”, *Neurocomput.*, **394**, 41-50. <https://doi.org/10.1016/j.neucom.2020.01.106>.
- Yu, Y., Li, Y., Li, J. and Gu, X. (2016), “A hysteresis model for dynamic behaviour of magnetorheological elastomer base isolator”, *Smart Mater. Struct.*, **25**(5), 055029. <https://doi.org/10.1088/0964-1726/25/5/055029>.
- Yu, Y., Rashidi, M., Samali, B., Mohammadi, M., Nguyen, T.N. and Zhou, X. (2022b), “Crack detection of concrete structures using deep convolutional neural networks optimized by enhanced chicken swarm algorithm”, *Struct. Health Monit.*, **21**(5), 14759217211053546. <https://doi.org/10.1177/14759217211053546>.
- Yu, Y., Samali, B., Rashidi, M., Mohammadi, M., Nguyen, T. N. and Zhang, G. (2022a), “Vision-based concrete crack detection using a hybrid framework considering noise effect”, *J. Build. Eng.*, **61**, 105246. <https://doi.org/10.1016/j.jobe.2022.105246>.
- Zhang, L., Ding, S., Li, L., Dong, S., Wang, D., Yu, X. and Han, B. (2018), “Effect of characteristics of assembly unit of CNT/NCB composite fillers on properties of smart cement-based materials”, *Compos. Part A Appl. Sci. Manuf.*, **109**, 303-320. <https://doi.org/10.1016/j.compositesa.2018.03.020>.
- Zhao, X.L., Bai, Y., Al-Mahaidi, R. and Rizkalla, S. (2014), “Effect of dynamic loading and environmental conditions on the bond between CFRP and steel: state-of-the-art review”, *J. Compos. Constr.*, **18**(3). [https://doi.org/10.1061/\(asce\)cc.1943-5614.0000419](https://doi.org/10.1061/(asce)cc.1943-5614.0000419).